© 2019. Published by The Company of Biologists Ltd | Journal of Experimental Biology (2019) 222, jeb176263. doi:10.1242/jeb.176263

RESEARCH ARTICLE

Avoiding topsy-turvy: how Anna's hummingbirds (*Calypte anna*) fly through upward gusts

Marc A. Badger[1,*], Hao Wang[2] and Robert Dudley[1]

ABSTRACT

Flying organisms frequently confront the challenge of maintaining stability when moving within highly dynamic airflows near the Earth's surface. Either aerodynamic or inertial forces generated by appendages and other structures, such as the tail, may be used to offset aerial perturbations, but these responses have not been well characterized. To better understand how hummingbirds modify wing and tail motions in response to individual gusts, we filmed Anna's hummingbirds as they negotiated an upward jet of fast-moving air. Birds exhibited large variation in wing elevation, tail pitch and tail fan angles among transits as they repeatedly negotiated the same gust, and often exhibited a dramatic decrease in body angle (29±6 deg) post-transit. After extracting three-dimensional kinematic features, we identified a spectrum of control strategies for gust transit, with one extreme involving continuous flapping, no tail fanning and little disruption to body posture (23±3 deg downward pitch), and the other extreme characterized by dorsal wing pausing, tail fanning and greater downward body pitch (38±4 deg). The use of a deflectable tail on a glider model transiting the same gust resulted in enhanced stability and can easily be implemented in the design of aerial robots.

KEY WORDS: Aerodynamics, Gust traversal, Flight control, Transit strategy, Perturbation, Stability

INTRODUCTION

Natural aerial environments are highly dynamic, with variable airflows deriving from vegetational interactions, wind shear and weather systems, and occurring on time scales ranging from fractions to many multiples of a characteristic wingbeat period. Gusts, turbulence and variable winds challenge both animals and small flying vehicles (Hoblit, 1988; Suomi et al., 2013). Turbulence can limit maximum forward flight speed in orchid bees (Combes and Dudley, 2009), and other insects flying within turbulent flows exhibit increased variance in body translation and rotation (Ravi et al., 2013; Ortega-Jimenez et al., 2013). Hummingbirds flying either in von Kármán vortex streets (Ortega-Jimenez et al., 2014) or in homogeneous free-stream turbulence (Ravi et al., 2015) compensate via highly variable wing and body kinematics, and intermittently fan the tail to effect stability. Flying in sustained turbulence is also known to increase the energetic costs of flight, especially at higher flight speeds (Bowlin and Wikelski, 2008).

Within forest canopies, gusts are frequently stronger than the mean wind speed and occur at frequencies relevant to flight control (0.2–0.3 Hz; McCay, 2003). The standard deviation of wind speed in rain forests is usually near the mean flow speed (0.2–0.3 m s^{-1}; McCay, 2003; Kruijt et al., 2000), but can be two to four times mean flow speed in boreal forests (2.1–2.5 m s^{-1}; Amiro, 1990). Although the general flow characteristics in some forests have been well studied, much less is known about how animals negotiate the unsteady, but structured, regions directly downstream of complex, porous obstacles characteristic of vegetation (Basnet, 2015; Wang and Takle, 1995). Behind such obstacles, flying animals traverse spatially adjacent regions characterized by low and high free-stream turbulence, von Kármán vortex streets and relatively still air in recirculation zones within just a few seconds. Whether wind transients result from gusts or from transitions between flow regions, animals necessarily experience substantial changes in local flow over their control surfaces.

Flight responses to wind transients, in contrast to turbulence, is much less studied, although ventral wing tucks have been identified for a large eagle flying through headwind gusts (Gillies et al., 2011; Reynolds et al., 2014) and insects demonstrate rapid kinematic responses to air puffs, typically using asymmetric responses in stroke amplitude (Vance et al., 2013). In response to gusts from various orientations, bumblebees (*Bombus ignitus*) exhibit rapid changes in body orientation primarily about the roll axes (Jakobi et al., 2018). Volant taxa must fly under a diversity of atmospheric conditions, and the range of transient responses is likely to be similarly variable and taxon-dependent. One of the problems of studying such rapid and unsteady aerial tasks is that of standardization; the temporal and spatial structure of the physical challenge as well as patterns of animal behavior can be difficult to repeat systematically within an experimental context. In this regard, the flight of hummingbirds presents a unique opportunity, given that their obligate nectar-feeding habits enable a high level of repeatability for spatially constrained flight trajectories if they are given suitable reward. Multiple transits of the perturbation per individual can thus be obtained using similar starting dynamic conditions.

Here, we challenged Anna's hummingbirds (*Calypte anna*) to fly through an artificial vertical gust of air and measured both wing and body kinematics as they transited this disturbed region. We identified a spectrum of behavioral responses, with one extreme dominated by continuous wing flapping and almost no tail fanning (which we refer to as wings-dominated) and the other by tail fanning with stationary, dorsally elevated wings (which we refer to as tail-dominated). We test the hypotheses that the outcome of a transit, as measured by the minimum body angle before recovery and transit speed, depends on both (i) entry conditions such as transit number, entry speed and initial body angle and (ii) motions of the wings and tail within the gust. Finally, we demonstrate that a rigid glider of comparable mass and with a bio-inspired and passively deflectable tail can successfully negotiate the same gust.

[1]Department of Integrative Biology, University of California, Berkeley, Berkeley, CA 94720, USA. [2]College of Astronautics, Nanjing University of Aeronautics & Astronautics, 29 Yudao St., 210016 Nanjing, China.

*Author for correspondence (badger@berkeley.edu)

M.A.B., 0000-0002-6411-706X; H.W., 0000-0003-2835-3839; R.D., 0000-0003-3707-5682

Received 17 December 2017; Accepted 5 December 2018

Journal of Experimental Biology (2019) 222, jeb176263. doi:10.1242/jeb.176263

MATERIALS AND METHODS

Animals and flight arena

Flights were recorded from a total of four adult male Anna's hummingbirds [*Calypte anna* (Lesson 1829), mean body mass of 4.46 g, wingspans 11.7, 11.2, 11.1 and 11.8 cm]. Birds were captured using a drop trap in Berkeley, CA, USA, and were housed in separate 1×1×1 m mesh cages. For experiments, individual birds were placed inside a mesh flight arena (30×40×130 cm, width×height×length) with an artificial flower at one end and a perch (30 cm from the mesh of the arena floor) at the other (Fig. 1C). A vertically oriented air knife (6″ Super Air Knife, model 110003, Exair Corp., Cincinnati, OH, USA) was positioned in the center of

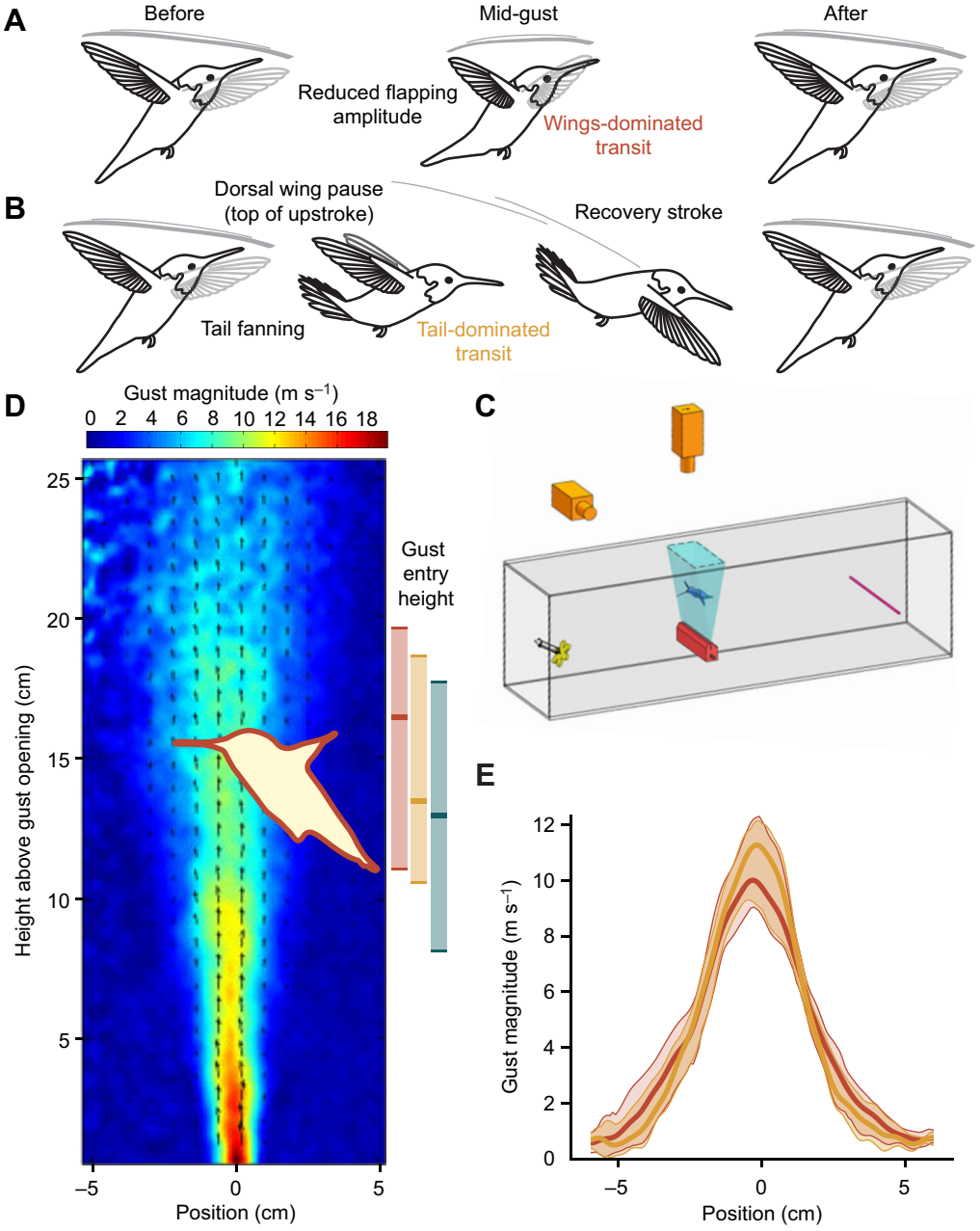

Fig. 1. Experimental setup, gust characterization and qualitative gust traversal methods used by Anna's hummingbirds. Two general methods are used in gust traversal: (A) the wings-dominated case, during which the wings are continuously flapped and tail fanning is limited, and (B) the tail-dominated case, in which the wings are held stationary at the top of upstroke with variable tail fanning, and with wing flapping resuming post-traversal. In most wings-dominated transits, the minimum body angle occurred during gust traversal; for most of the tail-dominated cases, minimum body angle occurred post-traversal (P<0.001). (C) Diagram of the flight arena. The gust generator (in red) was located at bottom center of a 130 cm long×30 cm wide×40 cm high mesh arena. Two high-speed cameras were mounted orthogonally at 80 cm above and lateral to the gust disturbance. Hummingbirds were trained to fly through the inactive disturbance zone (in blue) between the perch and nectar source before the gust generator was turned on. (D) Averaged velocity vector field of the air jet, with a hummingbird outline at typical entry height overlaid for scale. Red, yellow and green bars to the right show mean and 5th and 95th percentile entry heights for wings-dominated (n=5, 19, 23, 1 for birds 1–4, respectively), tail-dominated (n=6, 1, 0, 20) and control transits (n=5, 5, 2, 6), respectively. (E) Mean airspeed profile along the horizontal axis at the corresponding entry height for all wings- and tail-dominated transits (shown by thick red and yellow lines, respectively). Shading between thin lines indicates the 5th to 95th percentile of gust magnitude experienced by birds among all transits for each strategy, based on the range of gust entry heights shown in D.

Journal of Experimental Biology (2019) 222, jeb176263. doi:10.1242/jeb.176263

the flight arena; when activated by a constant air pressure (18 psi=124 kPa), this device produced a wedge of fast-moving air (Fig. 1D,E) that was nominally uniform along the crosswise axis of the arena. The flow field produced by the air knife was quantified with particle image velocimetry (PIV) using an identical setup previously described by Ortega-Jimenez et al. (2014). Along the long axis of the arena ('position', Fig. 1D,E), gust intensities greater than 1 m s^{-1} were only observed within a region approximately 10 cm wide at the typical entry height of the birds. At the center of the gust, upward flows ranged from 6 to 12 m s^{-1} depending on the height above the gust opening. Following Bernoulli's equation ($½\times\rho\times u^2+p$=constant, where ρ is air density, u is air flow speed and p is static pressure), the static pressure at the stagnation point on the underside of a crossing bird ranged from 0.022 to 0.088 kPa [=½×1.225 kg m^{-1}×(6 to 12 m s^{-1})^2].

Filming and kinematic analysis

Birds within the flight arena volitionally flew from the perch to feed at the flower, and then returned to the perch. Following a 2-min period of habituation after initial release in the arena, the air knife was turned on while the bird was on the perch. The gust remained on for the duration of the experiment. After a bird had completed a minimum of five consecutive transits, a series of flights through the gust in both directions was recorded using two orthogonally positioned high-speed video cameras (HiSpec1 2G Mono, Fastec Imaging Corporation). The first five gust transits were excluded from analysis to eliminate potentially atypical responses exhibited by birds during the first few transits (see Movie 1 for an example of a first transit by a pilot bird not used in this study). Our results therefore represent transit behaviors by birds potentially acting with full knowledge of the presence of the gust. We include transit number as a covariate in all statistical analyses to capture any learning that occurred after the initial transits. Synchronized videos were recorded at 500 Hz, and with a shutter speed of 200 µs. Videos were saved and evaluated in an uncompressed AVI format.

Landmarks on birds (Fig. 2) were digitized in each frame using DLTdv5 (Hedrick, 2008) and wing and body kinematics were reconstructed in three dimensions with custom MATLAB (MathWorks) scripts (Badger et al., 2018). The base of the beak and base of the tail were used to define the body longitudinal axis (i.e. the x-axis), with the beak base treated as the origin of the body-fixed coordinate system. The z-axis of the body was aligned in the sagittal plane perpendicular to the x-axis, and the y-axis was then determined using the right-hand rule. Flapping motion of the wings was characterized using three angles: the elevation angle (θ), sweep angle (ϕ) and rotation angle (ψ) about an axis connecting the wing base and wing tip (Fig. 2). The elevation angle is positive when the wing span axis lies dorsally, whereas the sweep angle is positive when the wing span is positioned anteriorly. The wing rotation angle was defined to be positive when the leading edge of the wing surface plane (defined by three landmarks: the wing base, wing tip and the tip of primary feather 4; see Fig. 2B) was rotated upwards relative to the horizontal. Pitch of the body relative to the global horizontal (χ; Fig. 2A) is positive when the body pitches up. Deflection of the tail (i.e. the tail elevation angle) was estimated as the angle between a vector from the tail base to the central tip of the tail and the horizontal plane (Fig. 2A) and is positive when the tail deflects upwards. The tail fan angle was estimated from the landmarks of the tail base and the lateral tip of the tail (Fig. 2B) and was calculated as the angle between the vectors from tail root to tail center and from tail root to lateral tip. The wingspan of each bird was estimated from 3D position data as twice the combined length from the wing tip to the wing base to the midline.

Filmed gust transits from the four birds yielded trajectory data for 11, 20, 23 and 21 gust transits and for 5, 5, 2 and 6 control transits for the four birds, respectively (93 transits in all). For each transit, minimum pitch angular acceleration, minimum body angle attained following gust transit, and transit duration were used to quantify the overall effects of the perturbation. Transits were divided into several time bins. Bin edges were set to the start of the video, when the bill base entered the edge of the gust, when the bill base crossed the midline of the gust, when the tail center crossed the midline of the gust, when the tail center left the edge of the gust, and the end of the video. Transit duration was calculated as the time between when the bill base crossed the midline to when the tail left the gust, as most aerodynamic surfaces of the bird were within the region of high upward flow during this period. Transits were aligned in time by the moment when the beak base crossed the virtual centerline of the gust (see Fig. S1). Mean wing kinematics during the gust were calculated over the duration of transit and tail elevation and fan angles were calculated over the period between when the tail center crossed the midline of the gust

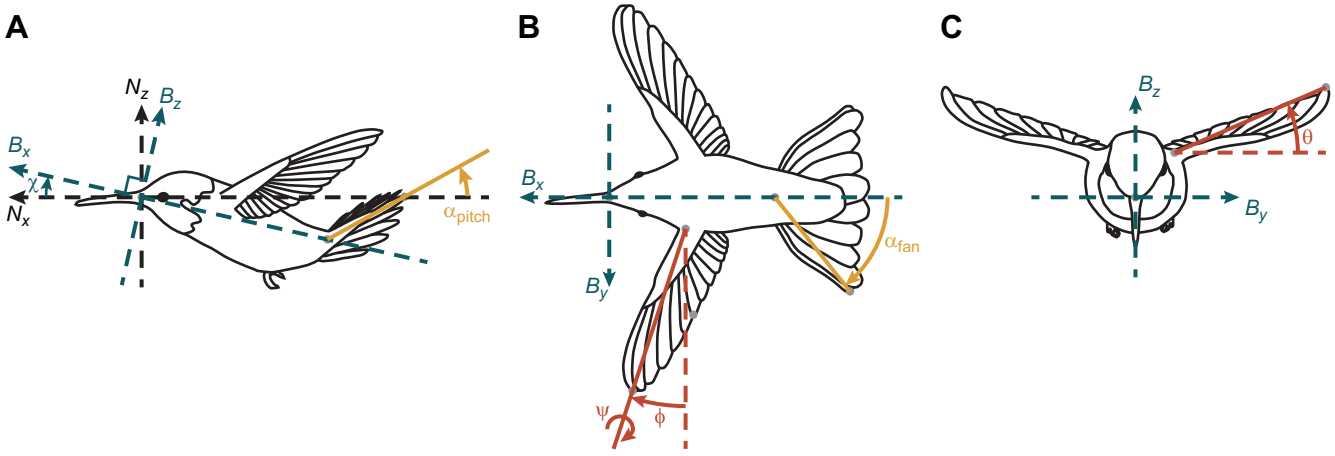

Fig. 2. Kinematic parameters and body and wing landmarks (gray points) used in digitization. (A) Lateral view of a hummingbird showing the vertical (N_z, B_z) and forward (N_x, B_x) axes in the global and body-fixed coordinate systems, respectively, along with the body angle (χ, in green) and tail deflection angle (α_{pitch}, in yellow). (B) Dorsal view of hummingbird showing angles of wing sweep (ϕ, in red), wing span rotation (ψ, in red), and the tail extension angle (α_{fan}, in yellow). (C) Frontal view of a hummingbird in the body coordinate system showing wing elevation angle (θ, in red).

to when it left the gust. For each transit, a dorsal wing pause ratio was also defined as the ratio of the duration that wings were both elevated and held posteriorly (i.e. elevation angle >0 deg and sweep angle <0 deg; see Figs 1B and 2) relative to the duration of each transit.

Statistics

The effects of the gust on the birds' behavior, mid-gust responses and flight trajectories were analyzed using general linear models. We parameterized behavior just prior to gust entry using height above the gust opening, horizontal flight speed, flight path angle, wing phase and initial body angle, which we generally refer to as 'gust entry variables' (Table S1). To assess the effect of bird ID, flight direction, transit number and the presence of the air gust (hereafter 'experimental variables') on each gust entry variable, we fit generalized least-squares models using the 'nlme' package in R (Fraley et al., 2012; Fraley and Raftery, 2002; https://cran.r-project.org/web/packages/nlme/index.html). Wing phase at gust entry was tested using an ANOVA for circular data using the package 'circular' (https://cran.r-project.org/web/packages/circular/index.html). Bird ID, flight direction and the presence of the air gust were included as categorical predictors and transit number (scaled to −0.5 to 0.5 within each bird ID×gust treatment combination) as a continuous predictor. Coefficients for the interactions of the air gust with bird ID, flight direction and transit number, and the interaction of bird ID with transit number were also estimated. Some fits showed unequal variance between gust-on and gust-off treatments, across levels of bird identity and with entry height. In these cases, the model with the minimum corrected Akaike's information criterion (AICc) was selected from a list of several models including various forms of heteroscedasticity as weights using varIdent and varPower variance functions [e.g. varPower(form=∼entryHeight|Gust) would model unequal variance across entry height at both levels of the gust variable; Pinheiro and Bates, 2000]. For variables that varied significantly with bird ID, we report significant differences among birds obtained from simultaneous tests for general linear hypotheses *post hoc* tests using the 'multcomp' (Hothorn et al., 2008) and 'emmeans' (https://cran.r-project.org/web/packages/emmeans/index.html) packages. Reported *P*-values are for likelihood ratio tests between a full model including all main effects and an identical model missing the corresponding effect of interest. We investigated the effects of the experimental variables on five 'technique variables' including tail elevation and fan angles, wing elevation and sweep angles, and percent dorsal wing pausing in the same manner. Finally, using the subset of transits for which the gust was on, we conducted two tests related to our hypotheses about whether performance variables (minimum body angle before recovery, minimum pitch angular acceleration and transit duration) were affected by either (i) gust entry variables or (ii) mid-gust behavior characterized by the five technique variables.

We tested these last hypotheses using a graphical model approach. We first assessed the effect of entry variables on performance variables regardless of technique. Because entry, technique, and performance variables varied significantly among individuals, we first controlled for bird ID, flight direction and transit number (i.e. we obtained the residuals, rE, rT and rP, of linear models with the experimental variables as predictors and entry, technique and performance variables as responses). In the graphical model approach, testing the independence of entry and performance variables is equivalent to testing for the presence of potential indirect effects of entry variables that are mediated through technique, rE→rT→rP, and/or direct effects, rE→rP, where rE, rT and rP correspond to the residuals of the fits for entry, technique and performance variables, respectively, and arrows indicate direct causal effects. Specifically, for each pair of entry (rE) and performance variables (rP), we performed a likelihood ratio test between a full model, rP∼BirdID+rE, and a reduced model rP∼BirdID.

To test the hypothesis that mid-gust behavior affects the resulting trajectory, we first noted that any observed relationship between technique on performance could potentially arise from direct dependence on entry or experimental variables alone (similar to the third-cause fallacy). We tested whether this was the case by first fitting linear models for both technique and performance variables to the entry variables (i.e. rT∼BirdID+rZB+rVX+rAN+rIBA and rP∼BirdID+rZB+rVX+rAN+rIBA, where ZB, VX, AN and IBA correspond to entry height, horizontal entry speed, entry path angle and initial body angle at entry, respectively) and collecting the residuals of these models, rrT and rrP. If there were a direct effect of technique on performance, then rrT and rrP would be significantly correlated, which we assessed using a Pearson's product-moment correlation test. When deciding which variables to include in these models, we made the *a priori* assumption that the physical process of how wing and body kinematics displayed within the gust influence the resulting trajectory does not depend on bird ID because other physical and morphological factors not captured by wing and body kinematics (e.g. sex and size) were very similar among birds. All *P*-values were corrected for false discovery rate (Benjamini and Yekutieli, 2001). Residuals of all models except for those corresponding to tail angle satisfied normality assumptions.

To assess whether gust responses could be better understood as discrete clusters, we clustered gust entry height, initial body angle, initial wing phase, tail fan and elevation angles, wing sweep and elevation angles, average speed during transit, minimum body angle, and minimum pitch angular acceleration into discrete strategies using Gaussian mixture models in the 'mclust' package in R (Fraley et al., 2012; Fraley and Raftery, 2002). The number of mixture components, as well as the size, axes and shape of the distributions, were selected by choosing the model with the maximum Bayesian information criterion value.

Glider model

A mechanical glider (Fig. 3) was built from balsa wood with a total mass of 2.6 g, length of 15.3 cm and wingspan of 15.0 cm (the wingspan of *C. anna* is 11–12 cm). In some trials, weight was added so that the mass (4.3 g) was comparable to that of male Anna's hummingbirds (4–6 g). The 3D trajectories with this additional mass were qualitatively similar, so we present data only for the lighter glider here. The tail area (430 mm^2) was intermediate to a typical hummingbird's folded (∼200 mm^2) and fully fanned tail (∼500 mm^2). A counterweight near the front of the glider was used to adjust the center of mass and to effect stable gliding.

The tail was mounted onto the body with a small hinge that enabled passive upwards deflection. A small magnet (11 mg) was embedded in the fuselage of the glider directly below the center of the tail. An identical magnet was glued to the bottom of the tail in line with the embedded magnet. The relative force required to deflect the tail was modulated by inserting either a third magnet or a balsa wood shim of the same thickness into the gap between the fuselage and tail magnets. The third magnet provided a strong enough attachment force that the tail did not deflect when hit by the gust. The balsa wood shim provided enough force to keep the tail fixed during normal flight, but it was easily deflected when the glider encountered the upward gust. The wings of the glider were rigidly mounted using stronger magnets. The glider was launched from a wooden platform

Journal of Experimental Biology (2019) 222, jeb176263. doi:10.1242/jeb.176263

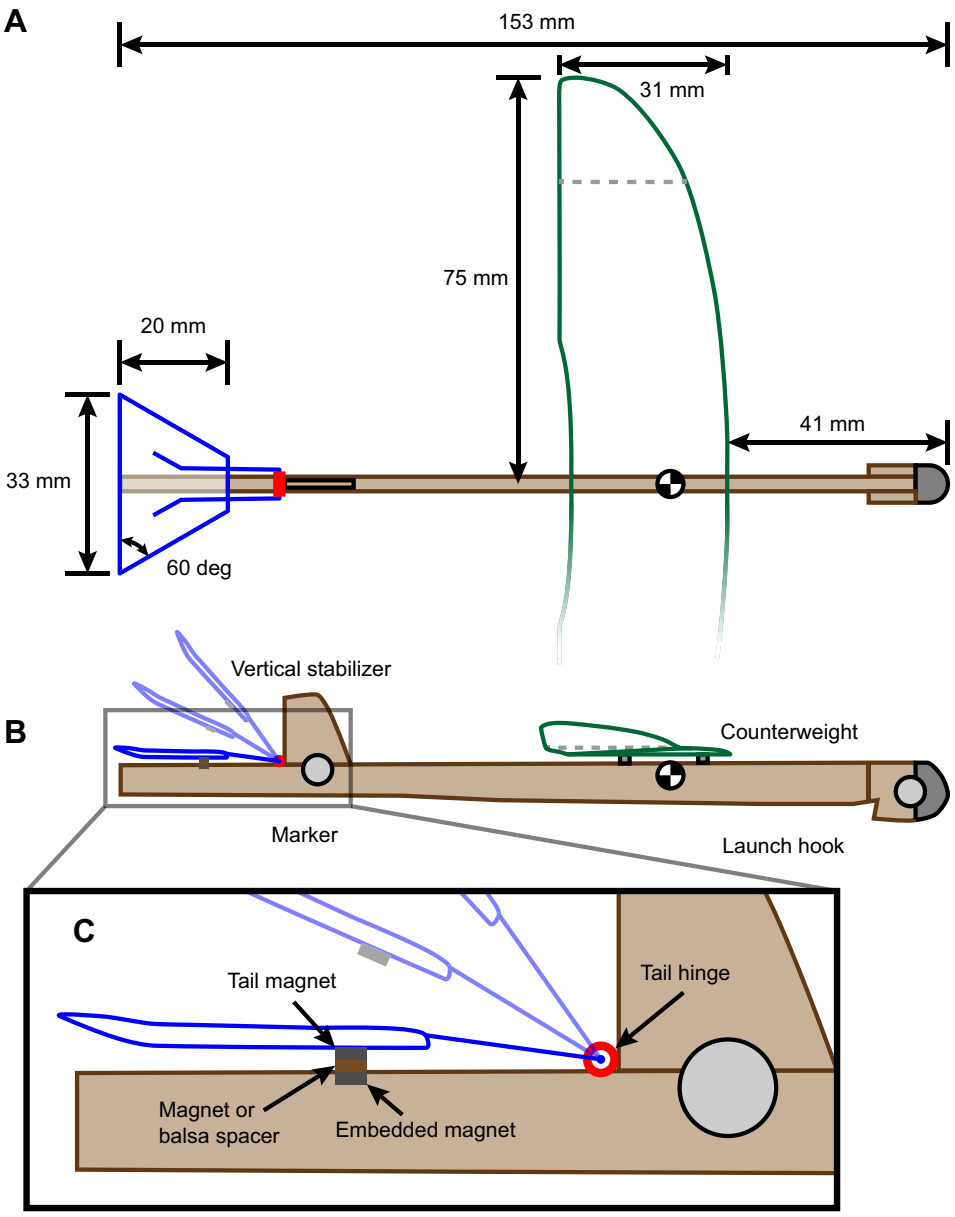

Fig. 3. Schematic diagram for a model glider capable of successfully traversing intense upward gusts. Top (A) and lateral views (B) of the glider depict how the tail (in blue) rotated passively around the hinge (in red) under aerodynamic forces imposed by the upward gust. Absent the gust and after gust transit, the tail was held fixed by the attracting force between the tail and embedded magnets (C). Attachment force was modulated by inserting either a third magnet, which prevented the gust from deflecting the tail, or a balsa spacer, which allowed the gust to deflect the tail (in brown). A counterweight near the front of the glider was used to adjust the center of gravity so as to effect stable flight.

with a rubber band stretched between two posts. The wooden platform was leveled with a calibrated iPhone inclinometer. The glider was drawn back to and released from the same location every trial, which ensured equivalent launch position and launch angle for all trials. Eight glides were recorded for each of four trial types: control (i.e. the wind gust was turned off) with both fixed and deflectable tail configurations, gust on with a fixed tail and gust on with a deflectable tail. Trials were filmed at 500 frames s^{-1} using three high-speed cameras. Two cameras had wide-angle (25 mm) lenses while the third had a zoomed (50 mm) lens, which provided a close-up of the tail motion during transit. Cameras were calibrated using functions provided with MATLAB and the Computer Vision System Toolbox (release 2016a, MathWorks). Trajectories of the front and rear markers were reconstructed in three dimensions, and the tail pitch angle was obtained from the close-up camera.

Ethics

The Animal Care and Use Committee at the University of California, Berkeley, whose activities are mandated by the US Animal Welfare Act and Public Health Service Policy, approved all experimental procedures (protocol AUP-2014-09-6676).

RESULTS

Flight through upward gusts causes large decreases in body angle

Transits through the gust perturbation resulted in extreme decreases in body pitch relative to control transits. Mean minimum body angle decreased from 21.1 deg for control transits to 4.5 deg for those when the air gust was on (a 16.6 deg decrease, $P<0.001$). Although both minimum body angle and the effect of the air gust on minimum body angle varied with bird identity ($P_{birdID}<0.001$, $P_{birdID:gust}<0.001$), the presence of the air gust decreased minimum body angle in all birds ($\beta_{gust}=-31.0$, -7.6, -3.2 and -24.5 deg for the four birds, respectively). Birds also flew much more slowly through the gust (mean transit duration 72.3 ms) than during control transits (mean transit duration 46.2 ms, $P<0.001$). As with minimum body angle, transit duration varied significantly with bird identity, but the increase

relative to control transits did not vary significantly among birds (P_{birdID}<0.001, $P_{birdID:gust}$=0.8).

In the presence of the gust, birds altered initial horizontal speed, initial body angle and entry height above the gust relative to control transits. Initial horizontal speed was consistently (but not significantly) slower when the gust was on (1.35 m s^{-1}) than when it was off (1.74 m s^{-1}, P=0.061; β_{gust}=−0.7, −0.2, −0.4 and −0.2 m s^{-1} for the four birds, respectively) and varied significantly with bird identity (P_{birdID}<0.001). Initial body angle was higher when the gust was present (33.3 deg) than for control transits (26.6 deg, P=0.025) and decreased with transit number ($\beta_{transitNum}$= −7.4 deg per experiment or −0.74 deg per transit, $P_{transitNum}$=0.015). Initial flight path angle was not significantly related to the presence of the gust, bird ID, or trial number (P=0.09, 0.06 and 0.09, respectively). Finally, entry height increased from an average of 13.4 cm above the gust opening for control transits to 16.6 cm in the presence of the gust (P<0.001). Entry height also varied significantly among birds, but the increase in entry height in the presence of the gust was not significantly different among birds (P_{birdID}<0.001, $P_{birdID:gust}$=1.0). Mean jet speed (averaged spatially over the gust) for the lowest quartile of entry heights was 5.8 m s^{-1} (maximum of 11.9 m s^{-1}), whereas mean jet speed for the highest quartile of entry heights was 4.3 m s^{-1} (maximum of 9.5 m s^{-1}). Thus, for transits in the lowest quartile of entry heights (i.e. those closest to the gust opening), birds experienced overall gust speeds that were 35% higher (or 25% higher for peak magnitude) than for those in the highest quartile of entry heights.

After controlling for variation in entry variables and performance owing to bird ID (see Materials and Methods), only entry path angle significantly affected minimum body angle, and only very slightly ($\beta_{entryPathAngle}$=−0.06, 0.63, 2.6 and 0.94 for the four birds, respectively, P=0.033). Minimum body angle also increased slightly with entry height ($\beta_{entryHeight}$=3.3, 0.2, 2.8 and 0.3 deg cm^{-1} for the four birds, P=0.089). Minimum pitch acceleration in the gust decreased significantly with initial body angle (mean β_{IBA}=396 s^{-2}, P=0.010). Thus, trials in which birds entered the gust with a more upright body angle also showed more extreme downward pitch accelerations (i.e. peak downward pitching angular acceleration was larger in magnitude). Transit duration increased with entry height, but this relationship was expected because the gust diverged with height above the opening and the distance birds traveled within the gust therefore increased with entry height. Mean instantaneous transit speed (averaged over the transit duration) did not change with entry height (P=1.0).

Wings- and tail-dominated responses to upward gust perturbations

Hummingbirds used a spectrum of control strategies when transiting the vertical gust. We visually inspected raw trajectories plotted versus position along the tunnel and noticed two general extremes. In wings-dominated responses, wings were flapped mostly anterior to the wing base with low-amplitude strokes, and the tail was elevated, but remained unfanned or minimally fanned (Fig. 1A; Movie 1). Alternatively, in tail-dominated responses, wings were retracted posteriorly and held still above the body while the tail was simultaneously elevated and fanned (Fig. 1B; Movie 1). The wingbeat flapping cycle was then resumed following transit of the gust. The number of flapping cycles during transit ranged from 1 to 8 (mean±s.e.m.=2.7±0.14).

Dorsoventral deflection of the tail was observed in all gust transits (average body-relative upward deflection of 59 deg, from −18 deg for control transits to 41 deg for gust transits; P<0.001). Simultaneous downward pitching of the body increased tail deflection in the global frame to 73 deg (from 46 deg below to 28 deg above the horizontal plane). Although both tail angle (relative to the horizontal) and the effect of the air gust on tail angle varied significantly with bird ID (P_{birdID}<0.001, $P_{birdID:gust}$<0.001), the presence of the air gust increased tail angle in all birds (β_{gust}=100, 75, 37 and 81 deg for the four birds, respectively). Birds also fanned their tails more when transiting the gust (mean 18 deg) relative to control transits (mean 7.5 deg, P_{gust}<0.020, $P_{birdID:gust}$<0.001, β_{gust}=14.0, 3.4, 2.4 and 23.0 deg, for the four birds, respectively). Tail fanning decreased significantly with transit number ($\beta_{transitNum}$=−7.7 deg per experiment or −0.73 deg per transit, P=0.018). Mean wing position variables during transit were not significantly different from those of controls (P=1 and β_{gust}=0.03% for dorsal wing pausing; P=1 and β_{gust}=−6.3 deg for mean wing sweep angle; P=0.069 and β_{gust}=8.0 deg for mean wing elevation angle). The phase of the wing stroke cycle at gust entry was not significantly different with either the presence of the gust (ANOVA for circular data, χ^2=0.03, d.f.=1, P=0.86) or bird ID (χ^2=5.02, d.f.=3, P=0.17).

Tail fanning is associated with larger decreases in body angle

We hypothesized that a bird's wing and tail motions within the gust would moderate the overall response to the air gust perturbation. We assessed the direct effect of technique variables (tail fan and pitch angles, wing elevation and sweep angles, and dorsal wing pausing) on performance variables (minimum body angle, minimum pitch acceleration and transit duration) for the subset of transits for which the gust was present. We first controlled for variation in technique and performance variables owing to bird ID and gust entry variables by obtaining residuals from a series of general linear models (see Materials and Methods). These residuals were then used to assess associations between technique and performance variables. Tail fanning was associated with lower (more extreme) minimum body angle (r=−0.43, −0.37, −0.47 and −0.37 for the four birds; mean r=−0.35, t=−3.2, d.f.=73, P=0.040; Fig. 4A) and lower (more extreme) minimum pitch acceleration (r=−0.08, −0.37, −0.60 and −0.49 for the four birds; mean r=−0.39, t=−3.7, d.f.=73, P=0.010; Fig. 4C). Increases in tail elevation angle relative to the horizontal were associated with lower minimum body angle (r=−0.50, −0.67, −0.45, −0.58 for the four birds; mean r=−0.55, t=−5.6, d.f.=73, P<0.001; Fig. 4B) and lower minimum pitch angular acceleration (r=−0.18, −0.58, −0.18 and −0.54 for the four birds; mean r=−0.37, t=−3.4, d.f.=73, P=0.024; Fig. 4D). Thus, both tail fanning and tail elevation were associated with more extreme downward pitch acceleration and more inclined downward body angles. Finally, greater wing sweep angle in the gust was associated with longer transit duration (r=0.41, t=3.8, d.f.=73, P=0.006). Wing elevation angle, wing sweep angle and dorsal wing pausing were all highly correlated (|r|>0.51 and P<0.001 in all cases).

Transits cluster into wings-dominated, tail-dominated and control strategies

We also assessed whether control kinematics and gust maneuvers fell into discrete strategies. A maximum Bayesian information criterion Gaussian mixture model incorporating gust entry height, initial body angle, initial wing phase, tail fan and elevation angles, wing sweep and elevation angles, average speed during transit, minimum body angle, and minimum pitch angular acceleration data partitioned maneuvers into three strategy clusters (grey ellipses in Fig. 5A–D). Clusters were most clearly separated by tail fan and

Journal of Experimental Biology (2019) 222, jeb176263. doi:10.1242/jeb.176263

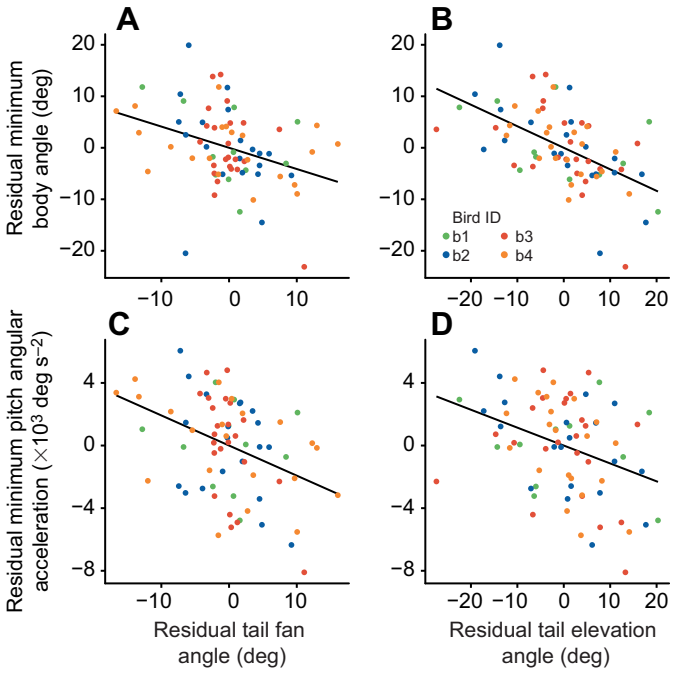

Fig. 4. Tail fanning and elevation significantly decreased minimum body angle and pitch angular acceleration of hummingbirds when transiting an upward gust. (A–D) After controlling for bird identity, transit direction, gust entry height and speed, and initial body angle (see Materials and Methods), greater tail fanning and higher tail upward elevation (i.e. a shift towards a tail-dominated strategy) significantly decreased minimum pitch angular acceleration (P<0.001 and P=0.025 for fanning and elevation, respectively; C,D) resulting in a much larger pitching response to the perturbation (P=0.040 and P<0.001 for fanning and elevation, respectively; A,B). Number of gust-on transits is n=11, 20, 23, 21, for birds 1–4, respectively.

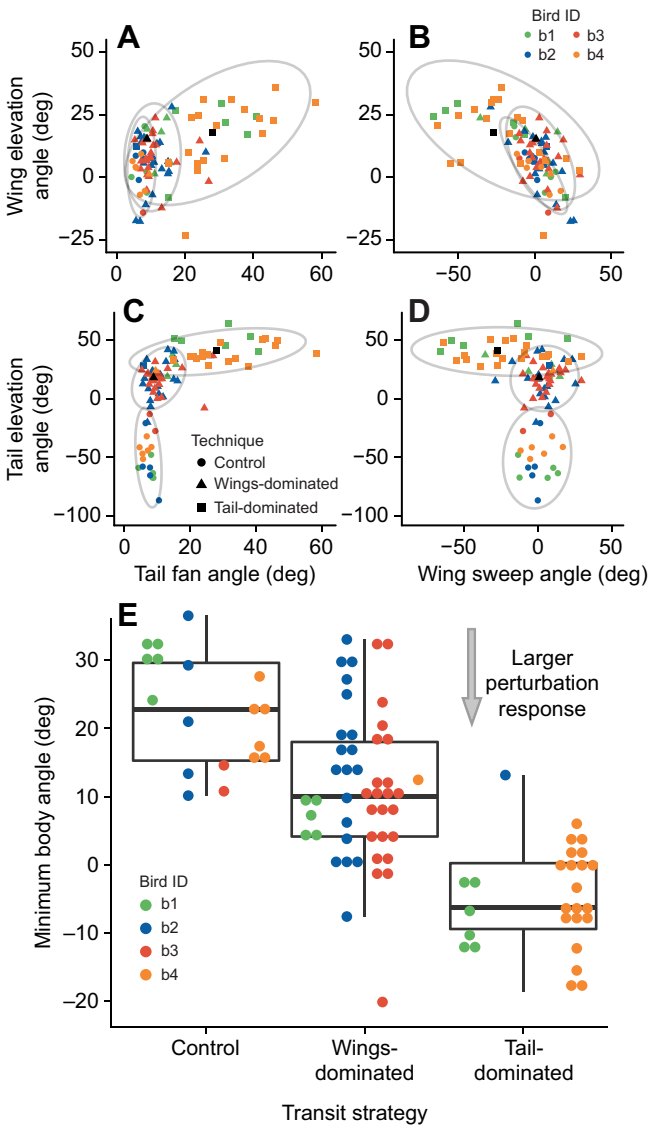

Fig. 5. Mean wing and tail angles of hummingbirds while transiting upward gusts vary widely among both transits and birds. (A–D) Wing and tail kinematics data were classified into transit strategy clusters using Gaussian mixture models (see Materials and Methods), with the number of clusters selected using the Bayesian information criterion. Each point corresponds to one transit. Point shape corresponds to the most probable cluster (gray ellipses) and point color corresponds to bird identity. The 'control' cluster (circles) is completely composed of control transits for which the gust was turned off, and no other cluster contains control transits. Note that clusters appear to overlap because data points and clusters are projected from several dimensions onto two. Black squares and triangles represent the tail- and wings-dominated example transits shown in Movie 1. (E) Relative to control transits, gust transits resulted in large downward pitching rotations of the body. Each point represents a single transit, colored by bird identity, and boxplots depict all transits for a given technique. Gust-associated pitching was more pronounced (i.e. a lower minimum body angle) for the tail-dominated response than for the wings-dominated response. For transits in the presence of the gust, birds 2 and 3 almost always used the wings-dominated response, and bird 4 almost always used the tail-dominated response. See Results and Fig. 4 for statistical tests and Fig. S3 for additional comparisons.

elevation angles (Fig. 5C). The control cluster was characterized by the distinct combination of low tail fanning (mean 7.3 deg, range 4.3–11 deg) and tail elevation angle (mean −50 deg, range −87 to −13 deg), but also had higher (less extreme) minimum body angles (mean 23 deg, range 10–37 deg; Fig. 5E) and minimum pitch angular acceleration (mean −76 deg s^{-2}, range −7500 to 6100 deg s^{-2}) than the other clusters (Table S2). All control transits were assigned to the control cluster and no gust-on transits were assigned to the control cluster. Like the control cluster, the wings-dominated cluster also had low tail fanning (mean 11 deg, range 5.3–27 deg), but was instead combined with high tail elevation angle (mean 17 deg, range −21 to 41 deg; triangles in Fig. 5C). The tail-dominated cluster (squares in Fig. 5C) was characterized by both high tail elevation angle (mean 41 deg, range 27–64 deg) and high tail fanning (mean 29 deg, range 5.7–58 deg). Transits in the tail-dominated cluster also had more elevated and swept wings than did transits in the control or wings-dominated clusters (squares in Fig. 5B,D; see Table S2 for means and ranges). Gust entry height for the tail-dominated cluster was lower than for the wings-dominated cluster (Fig. 1D; Fig. S3, Table S2).

The tail-dominated cluster also had the lowest entry speed, minimum body angle (Fig. 5E) and minimum pitch angular acceleration of the three clusters (Fig. S3, Table S2). In fact, when using the tail-dominated response, minimum body angle was usually attained only after passing through the gust (26 out of 27 transits), whereas minimum body angle for the wings-dominated response occurred within the gust much more frequently (14 out of 34 transits; Chi-square test, χ^2=5.5, P=0.019). Across birds and technique clusters, fanned and elevated tails usually appear concurrently with elevated and swept wings (i.e. when dorsal wing pausing is high). These results agree with those reported above for the regression analyses.

Journal of Experimental Biology (2019) 222, jeb176263. doi:10.1242/jeb.176263

Among-individual variation in transit strategy and performance

In the presence of the gust, significant differences among birds occurred for nearly all examined variables (P_{birdID}<0.009 for all variables except wing sweep), particularly between birds 2 and 4 and between birds 3 and 4. Compared with birds 2 and 3, bird 4 entered the gust 4.9 and 4.3 cm closer to the gust opening, respectively (multiple comparisons of means, P<0.001 for bird 4 versus 2 and bird 4 versus 3). In fact, bird 4 flew more than 4 cm (25%) closer to the gust on average than did any other bird. Bird 4 also fanned its tail 18 and 19 deg more than birds 2 and 3, respectively (P<0.001), elevated its tail 21 deg more (P<0.001), and swept its wings 22 deg more (P=0.008) and 23 deg more (P=0.028) than birds 2 and 3, respectively. The minimum body angle for bird 4 was also 18 and 14 deg lower (more extreme) than for birds 2 and 3, respectively (P<0.001; see Fig. S2A for body angle trajectories). Bird 3 transited the gust with an average speed 0.57 m s^{-1} (47%) faster than the average for the other three birds and experienced the smallest magnitude of pitch angular acceleration within the gust (blue trajectories in Fig. S2A). Bird 4 almost always used the tail-dominated response, whereas birds 2 and 3 almost always used the wings-dominated response (Fig. 5E). Over repeated transits, bird 2 (n=20 gust transits) decreased its tail fan and elevation angles, increased its minimum body angle and reduced the magnitude of downward pitch angular acceleration during the gust. These relationships between transit strategy and performance metrics over time match those found among and within birds above, but none of these trends were significant after adjusting for false discovery rate.

The analyses thus far have included an intercept for bird ID in the initial models used to control for experimental and gust entry variables. Because birds seem to vary somewhat systematically in their strategies and outcomes, however, these models could incorrectly attribute some variation to bird ID rather than to a potentially true relationship between gust entry and response variables, thereby reducing the apparent effect of gust entry and technique variables on gust negotiation performance. Repeating the above analyses without initially controlling for bird ID (thereby obtaining results reflecting both within- and among-bird variation) revealed qualitatively similar results, but with correlations slightly larger in magnitude.

A deflectable tail improves upward gust rejection in a model glider

The effectiveness of tail deflection in response to upward gusts was demonstrated empirically using a dorsally deflectable tail on a glider model (Figs 3 and 6). Gliders entered the gust with an average speed of 3.01±0.11 m s^{-1} (mean±s.d. for this and following results; about twice the typical entry speed of birds) following a downward path at an angle of 8.5±1.9 deg below the horizontal. Mean body angle upon entrance averaged −0.2±2.9 deg. These values did not differ significantly between the two control conditions (t-tests: entrance speed, P=0.76; entrance angle, P=0.69; entrance body angle P=0.37); control trials were thus pooled for subsequent trajectory analyses. Furthermore, entry trajectory metrics did not differ significantly between the fixed and deflectable tail treatments (t-tests: entrance speed, P=0.40; entrance angle, P=0.93; entrance body angle, P=0.39), nor did they differ significantly among the four experimental and control conditions (ANOVAs: entrance speed, P=0.094; entrance angle, P=0.422; entrance body angle, P=0.19).

Mean post-gust body angles (i.e. body angle between t=0.002 and t=0.344 s averaged within each trial) of the glider in the deflectable tail condition were not significantly different from those observed with the gust turned off, with the glider in either the deflectable (P=0.094; Movie 1) or fixed tail condition (P=0.79). Body angle decreased significantly (i.e. the body rotated nose downward) when the tail was held fixed (P<0.001; Fig. 6; Movie 1).

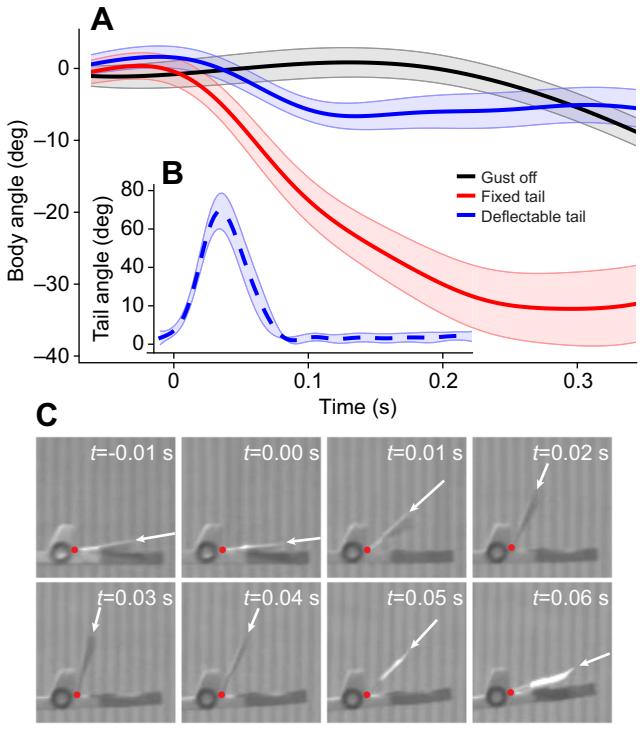

Fig. 6. A deflectable tail improves pitch stability of a glider traversing an upward gust. The glider is launched horizontally with a body angle near 0 deg. (A) Absent a vertical gust (in black), the glider exhibits only slight upwards and downwards changes in pitch. In a vertical gust, the glider with a fixed tail (in red) pitches up when its wings encounter the airflow (at about −0.03 s), but then dives when the tail encounters the gust (~0.00 s). The glider with a deflectable tail (in blue) avoids this downward pitching torque because the tail deflects upward with the gust (B,C). (C) Close-up view of the rear portion of the glider as the tail deflects upward after encountering the upward gust. In each frame, the axis of rotation and tail angle are shown by the red dot and white arrow, respectively. Initial glider angle did not differ among treatments (P=0.19), but the mean glider angle (i.e. body angle between t=0.002 and t=0.344 s averaged within each trial) following gust traversal was significantly lower for the fixed tail condition compared with either of the control conditions with no gust (P<0.001 in both cases) or with the deflectable tail (P<0.001). There was also no significant difference between the deflectable tail and either control treatment (P=0.094, P=0.79). Lines and colored bands indicate mean values and 95% confidence intervals (n=8 each for fixed and deflectable treatments, n=16 for control), respectively. All statistical tests are one-way ANOVAs with Tukey pairwise comparisons.

DISCUSSION

Gust rejection and recovery from gust-induced perturbations

Mid-air disturbance is commonplace for animals flying within the atmosphere, and requires compensatory kinematics. Here, hummingbirds traversed a thin region of air flowing upwards at ~10 m s^{-1}, more than six times the typical flight speed in the arena. Responses varied both among transits and among birds. In general, fanning of the tail was associated with larger downward deflections in body angle. The mean minimum body angle for the cluster of tail-dominated responses was 16 deg lower than for the cluster of wings-dominated responses (Fig. 5E). It remains unclear whether the observed increases in tail elevation and tail fan angle are caused directly by the gust or are part of a longer-term recovery strategy

(e.g. producing an upward aerodynamic torque or redirecting flow coming from the wings). Similarly, the average instantaneous flight speed within the gust was also 13% lower for the cluster of tail-dominated responses than for the wings-dominated cluster (1.28 versus 1.47 m s^{-1}; note this difference is driven almost entirely by differences in gust entry speed). Thus, the tail-dominated response, in which wings were held stationary behind the body and the tail was elevated and fanned, was associated with both slower flight and larger downwards pitching of the body. Despite these apparent drawbacks of the tail-dominated response, dorsal elevation of the transiently static wings in this strategy decreased the projected wing span relative to the oncoming flow, and likely also improved stability in roll and yaw (Hedrick et al., 2009). Pauses in flapping at the top of the upstroke have also been observed in pigeons negotiating arrays of vertical poles (Williams and Biewener, 2015). Following gust passage, body pitch was recovered via aerodynamic torques generated by the subsequent wingbeats. Similar to escape maneuvers, the majority of the pitching torque is likely produced during these recovery downstrokes (Cheng et al., 2016a,b). As in pigeons, exchange of angular momentum between the wings and body (i.e. an inertial effect of the wings; Ros et al., 2015) is unlikely to contribute substantially to body reorientation during recovery because the total mass of both wings is small compared with that of the body (~4%; Chai and Dudley, 1996) and mass within the wings is distributed near the root (Wells, 1990).

Advantages of dorsal wing pausing versus flapping

Although transit strategy varied with gust entry height, the distributions overlap considerably (Fig. 1D), indicating that gust intensity (which differed by ~35% between the lowest and highest quartiles of entry height) is not the only factor driving transit behavior. We observed significant, correlated variation among birds in entry height, mid-gust transit strategy and minimum body angle, particularly among birds 2, 3 and 4. The fact that among-bird patterns reflect the within-bird regression results suggests a similar underlying relationship between these variables. Although our sample size and number of transits collected per bird (11 to 23) did not show many significant trends over time, it is possible that birds would adjust entry, mid-gust and recovery behaviors over the course of hundreds of gust transits. Such experiential learning is expected to benefit hummingbirds following the same flight path dozens or hundreds of times per day. If birds can choose their transit strategy, the correlation of transit strategy with perturbation-induced pitching (Fig. 4A–D) may allow them to adjust their trajectory according to the relative costs of transit speed, body angle disruption and stress on the wings. One potential advantage of pauses in flapping with the wings held dorsally (Fig. 1B), as performed in the tail-dominated transit strategy, is that it may reduce the high torque on otherwise extended wings; in aircraft, gust load may yield wing-root bending moments that may cause the wing to fail (e.g. Hoblit, 1988; Moulin and Karpel, 2007). In contrast, flapping wings may themselves mitigate the aerodynamic effects of unexpected gusts because lift fluctuations are known to decrease as flapping frequency is increased (Fisher et al., 2016). These effects, along with the ability of hummingbirds to alter wing kinematics on a stroke-by-stroke basis (Cheng et al., 2016a), may explain why the wings-dominated technique is associated with a less pronounced pitch response.

The role of deflectable tails in gust rejection

Some dorsoventral deflection of the tail was observed in all gust transits and likely contributed to pitch control, as passive tail deflection on the mechanical glider yielded much higher stability (Fig. 6). We found that transits in which birds had a higher tail elevation angle also had a lower minimum body angle. This somewhat counter-intuitive correlation may indicate that the tail is being deflected passively and that unmodeled variation in the size of the gust perturbation may be simultaneously driving both tail and body responses. For active tails, computational modeling of steady-state forward flight for an ornithopter shows that periodic dorsoventral motions of the tail can reduce oscillations in body pitch (Lee et al., 2012). Because tail motions may involve lateral fanning as well as dorsoventral motion at variable amplitudes, a wide range of control strategies can potentially derive from a mobile tail, and deserve further investigation in both biological and technological contexts. For instance, bats likely modulate the angle of the tail membrane to produce pitching moments in flight (Gardiner et al., 2011). Caudal filaments characteristic of many insect taxa may serve a similar role in controlling (via abdominal flexion with filaments trailing passively) and stabilizing flight when transiently perturbed (Yanoviak et al., 2009). The tails and other trailing structures of birds, bats and insects are highly variable in size and shape, and likely serve a variety of mechanical functions (including stabilization and gust rejection) during both steady and maneuvering flight.

Considerations for future work

This study confronted hummingbirds flying horizontally with an isolated vertical gust of constant intensity, but animals can potentially experience aerial perturbations of variable magnitude, orientation and duration (Ortega-Jimenez et al., 2016). Further experiments will be needed to determine the gust orientations and intensity thresholds under which compensatory behaviors are induced. Such behaviors likely also depend on the size of the animal relative to the spatial extent of the gust as well as species-dependent morphology and flapping kinematics. The gusts and shear zones (up to 12 m s^{-1} change in speed over 2 to 3 cm) successfully transited by hummingbirds in this experiment may be at the upper limit of conditions they regularly encounter in the field. Hummingbirds encountering gusts of lower magnitude in the field should therefore exhibit less extreme responses, but we emphasize the need for more detailed measurements of the spatial and temporal variability of air flows at scales relevant to locomotion within and adjacent to vegetation.

Because the gust in this experiment was continuously active and kept at a fixed position within the enclosure, the observed responses may be different from those in less predictable environments. Flying animals that follow stereotyped routes during trap-lining, homing or other repetitive flight behaviors may benefit from knowledge about upcoming regions of consistent yet spatially variable flow (such as those downstream of stationary vegetation) by learning maneuvering strategies catered to the specific flow sequences experienced along the flight path (Stamps, 1995). In future work, it will be interesting to characterize the extent to which birds develop such maneuvering strategies and to investigate whether these maneuvers or postures differ from those used to transit regions with less predictable flows (e.g. regions downstream of swaying branches). Hummingbirds flying within von Kármán vortex streets (Ortega-Jimenez et al., 2014) and in freestream turbulence (Ravi et al., 2015) show standard deviations in wingbeat frequency, wing stroke amplitude and tail fan angle more than double those of control flights. Time-resolved responses to identifiable, yet unpredictable gusts have not yet been characterized, but it is likely that responses to multiple upward gusts would manifest as increases in the standard deviations of wing and tail kinematics across time. The responses presented here establish an upper limit on the detrimental effects of intense, localized wind gusts and demonstrate the strategies hummingbirds use to reject such gusts.

Given the wide range of potential aerial disturbances found in natural environments, together with the high level of morphological diversity seen among volant taxa (and particularly insects), many different control strategies using flexible wings and tails are possible. To date, only four other studies have addressed gust responses in volant taxa. Rapid headwind gusts induced ventral and bilaterally symmetric curling of the wings in a raptor (Reynolds et al., 2014), whereas flying insects exposed to continuous gusts (Jakobi et al., 2018) or rapid puffs of air (Vance et al., 2013) responded with asymmetric wing motions using both visual and mechanosensory information (Fuller et al., 2014). As demonstrated here, even simple implementation of a rigid but deflectable tail in a fixed-wing glider improved gust response. Flexible wings and tails, combined with variable kinematics, should thus yield a large and as yet undescribed set of control responses that could also be implemented in small flying machines.

Acknowledgements
We thank Kathryn McClain for prototyping the behavioral experiments and Xingbang Yan (Robotic Institute, Beihang University), Qingyu Mao, Man Ho Tang and Stacey Yu for help with data collection and/or digitizing of videos. Portions of the data and results in this paper were previously presented in the PhD thesis of M.B. (2016, University of California, Berkeley; permalink: https://escholarship.org/uc/item/5hz6m9fq). We also thank two anonymous reviewers for their helpful insights and constructive feedback.

Competing interests
The authors declare no competing or financial interests.

Author contributions
Conceptualization: M.A.B., R.D.; Methodology: M.A.B., H.W., R.D.; Software: M.A.B., H.W.; Validation: M.A.B., H.W.; Formal analysis: M.A.B., H.W., R.D.; Investigation: M.A.B., H.W., R.D.; Resources: M.A.B., R.D.; Data curation: M.A.B., H.W.; Writing - original draft: M.A.B., H.W.; Writing - review & editing: M.A.B., R.D.; Visualization: M.A.B., H.W.; Supervision: M.A.B., H.W., R.D.; Project administration: M.A.B., R.D.; Funding acquisition: M.A.B., H.W., R.D.

Funding
This work was supported by the Air Force Office of Scientific Research (Flow Interactions and Control grant 13RSA030) and by the National Natural Science Foundation of China (61375096). M.A.B was supported by a National Science Foundation CiBER-IGERT under Award DGE-0903711 and a National Science Foundation Graduate Research Fellowship under Grant No. DGE-1106400. Any opinion, findings, and conclusions or recommendations expressed in this material are those of the authors and do not necessarily reflect the views of the National Science Foundation.

Data availability
Data and analysis codes supporting this study are available from the Dryad Digital Repository (Badger et al., 2018): https://doi.org/10.5061/dryad.hm573.

Supplementary information
Supplementary information available online at
http://jeb.biologists.org/lookup/doi/10.1242/jeb.176263.supplemental

References
Amiro, B. D. (1990). Comparison of turbulence statistics within three boreal forest canopies. *Boundary Layer Meteorol.* **51**, 99-121.
Badger, M., Wang, H. and Dudley, R. (2018). Data from: avoiding topsy-turvy: how Anna's hummingbirds (*Calypte anna*) fly through upward gusts. *Dryad Digital Repository*.
Basnet, K. (2015). Flow around porous barriers: fundamental flow physics and applications. PhD thesis, University of Iowa, Iowa City, IA, USA.
Benjamini, Y. and Yekutieli, D. (2001). The control of the false discovery rate in multiple testing under dependency. *Ann. Stat.* **29**, 1165-1188.
Bowlin, M. S. and Wikelski, M. (2008). Pointed wings, low wing loading and calm air reduce migratory flight costs in songbirds. *PLoS ONE* **3**, e2154.
Chai, P. and Dudley, R. (1996). Limits to flight energetics of hummingbirds hovering in hypodense and hypoxic gas mixtures. *J. Exp. Biol.* **199**, 2285-2295.
Cheng, B., Tobalske, B. W., Powers, D. R., Hedrick, T. L., Wethington, S. M., Chiu, G. T. C. and Deng, X. (2016a). Flight mechanics and control of escape manoeuvres in hummingbirds I. Flight kinematics. *J. Exp. Biol.* **219**, 3518-3531.
Cheng, B., Tobalske, B. W., Powers, D. R., Hedrick, T. L., Wethington, S. M., Chiu, G. T. C. and Deng, X. (2016b). Flight mechanics and control of escape manoeuvres in hummingbirds II. Aerodynamic force production, flight control and performance limitations. *J. Exp. Biol.* **219**, 3532-3543.
Combes, S. A. and Dudley, R. (2009). Turbulence-driven instabilities limit insect flight performance. *Proc. Natl. Acad. Sci. USA* **106**, 9105-9108.
Fisher, A., Ravi, S., Watkins, S., Watmuff, J., Wang, C., Liu, H. and Petersen, P. (2016). The gust-mitigating potential of flapping wings. *Bioinspir. Biomim.* **11**, 046010.
Fraley, C. and Raftery, A. E. (2002). Model-based clustering, discriminant analysis and density estimation. *J. Am. Stat. Assoc.* **97**, 611-631.
Fraley, C., Raftery, A. E., Murphy, T. B. and Scrucca, L. (2012). mclust Version 4 for R: Normal mixture modeling for model-based clustering, classification, and density estimation. Technical Report No. 597, Department of Statistics, University of Washington.
Fuller, S. B., Straw, A. D., Peek, M. Y., Murray, R. M. and Dickinson, M. H. (2014). Flying *Drosophila* stabilize their vision-based velocity controller by sensing wind with their antennae. *Proc. Natl. Acad. Sci. USA* **111**, E1182-E1191.
Gardiner, J. D., Dimitriadis, G., Codd, J. R. and Nudds, R. L. (2011). A potential role for bat tail membranes in flight control. *PLoS ONE* **6**, e18214.
Gillies, J., Thomas, A. L. R. and Taylor, G. K. (2011). Soaring and manoeuvring flight of a steppe eagle *Aquila nipalensis*. *J. Avian Biol.* **42**, 377-386.
Hedrick, T. L. (2008). Software techniques for two- and three-dimensional kinematic measurements of biological and biomimetic systems. *Bioinspir. Biomim.* **3**, 034001.
Hedrick, T. L., Cheng, B. and Deng, X. Y. (2009). Wingbeat time and the scaling of passive rotational damping in flapping flight. *Science* **324**, 252-255.
Hoblit, F. M. (1988). *Gust Loads on Aircraft: Concepts and Applications*. AIAA Education Series. Washington, DC: AIAA.
Hothorn, T., Bretz, F. and Westfall, P. (2008). Simultaneous inference in general parametric models. *Biom. J.* **50**, 346-363.
Jakobi, T., Kolomenskiy, D., Ikeda, T., Watkins, S., Fisher, A., Liu, H. and Ravi, S. (2018). Bees with attitude: the effects of directed gusts on flight trajectories. *Biol. Open* 7, bio034074.
Kruijt, B., Malhi, Y., Lloyd, J., Norbre, A. D., Miranda, A. C., Pereira, M. G. P. and Culf, A. (2000). Turbulence statistics above and within two Amazon rain forest canopies. *Bound.-Layer Meteorol.* **94**, 297-331.
Lee, J.-S., Kim, J.-K., Han, J.-H. and Ellington, C. P. (2012). Periodic tail motion linked to wing motion affects the longitudinal stability of ornithopter flight. *J. Bionic. Engin.* **9**, 18-28.
McCay, M. G. (2003). Winds under the rain forest canopy: the aerodynamic environment of gliding tree frogs. *Biotropica* **35**, 94-102.
Moulin, B. and Karpel, M. (2007). Gust loads alleviation using special control surfaces. *J. Aricraft* **44**, 17-25.
Ortega-Jimenez, V. M., Greeter, J. S. M., Mittal, R. and Hedrick, T. L. (2013). Hawkmoth flight stability in turbulent vortex streets. *J. Exp. Biol.* **216**, 4567-4579.
Ortega-Jimenez, V. M., Sapir, N., Wolf, M., Variano, E. A. and Dudley, R. (2014). Into turbulent air: size-dependent effects of von Kármán vortex streets on hummingbird flight kinematics and energetics. *Proc. Biol. Sci.* **281**, 20140180.
Ortega-Jimenez, V. M., Badger, M. A., Wang, H. and Dudley, R. (2016). Into rude air: hummingbird flight performance in variable aerial environments. *Philos. Trans. R. Soc. Lond. B* **371**, 20150387.
Pinheiro, J. C. and Bates, D. M. (2000). *Mixed-Effects Models in S and S-PLUS*. Springer.
Ravi, S., Crall, J. D., Fisher, A. and Combes, S. A. (2013). Rolling with the flow: bumblebees flying in unsteady wakes. *J. Exp. Biol.* **216**, 4299-4309.
Ravi, S., Crall, J. D., McNeilly, L., Gagliardi, S. F., Biewener, A. A. and Combes, S. A. (2015). Hummingbird flight stability and control in freestream turbulent winds. *J. Exp. Biol.* **218**, 1444-1452.
Reynolds, K. V., Thomas, A. L. R. and Taylor, G. K. (2014). Wing tucks are a response to atmospheric turbulence in the soaring flight of the steppe eagle *Aquila nipalensis*. *J. R Soc. Interface* **11**, 20140645.
Ros, I. G., Badger, M. A., Pierson, A. N., Bassman, L. C. and Biewener, A. A. (2015). Pigeons produce aerodynamic torques through changes in wing trajectory during low speed aerial turns. *J. Exp. Biol.* **218**, 480-490.
Stamps, J. (1995). Motor learning and the value of familiar space. *Am. Nat.* **146**, 41-58.
Suomi, I., Vihma, T., Gryning, S. E. and Fortelius, C. (2013). Wind-gust parametrizations at heights relevant for wind energy: a study based on mast observations. *Q. J. R. Meteorol. Soc.* **139**, 1298-1310.
Vance, J. T., Faruque, I. and Humbert, J. S. (2013). Kinematic strategies for mitigating gust perturbations in insects. *Bioinspir. Biomim.* **8**, 016004.
Wang, H. and Takle, E. S (1995). A numerical simulation of boundary-layer flows near shelterbelts. *Boundary Layer Meteorol.* **75**, 141-173.
Wells, D. J. (1990). Hummingbird flight physiology: muscle performance and ecological constraints. *PhD thesis*, University of Wyoming, Laramie.
Williams, C. D. and Biewener, A. A. (2015). Pigeons trade efficiency for stability in response to level of challenge during confined flight. *Proc. Natl. Acad. Sci. USA* **112**, 3392-3396.
Yanoviak, S., Kaspari, M. and Dudley, R. (2009). Gliding hexapods and the origins of insect aerial behaviour. *Biol. Lett.* **5**, 510-512.